

Nearest Neighbors GParareal: Improving Scalability of Gaussian Processes for Parallel-in-Time Solvers

WARWICK
THE UNIVERSITY OF WARWICK

Guglielmo Gattiglio, Lyudmila Grigoryeva, Massimiliano Tamborrino
Department of Statistics, University of Warwick, Coventry, UK guglielmo.gattiglio@warwick.ac.uk

Motivation

Why is time parallelization for ODEs and PDEs important?

- In plasma physics and other fields, space parallelization reaches saturation on modern supercomputers leaving time parallelization as the only avenue for improvement [1].
- Simulations of molecular dynamics often involve averages over very long trajectories of stochastic dynamics [2].

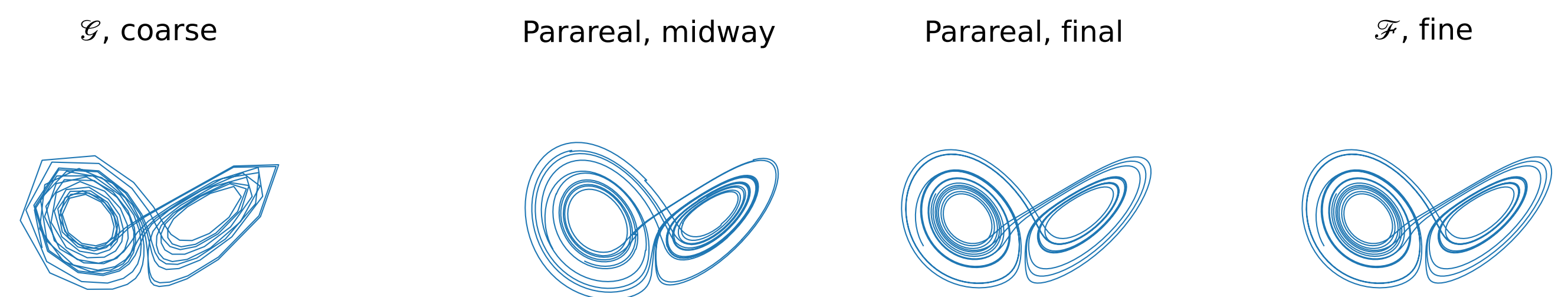


Figure 1: Visualization of Parareal evolution on chaotic Lorenz attractor.

Existing Approaches: Parareal and GParareal

Consider a system of $d \in \mathbb{N}$ ODEs (and similarly for PDEs)

$$\frac{du}{dt} = h(u(t), t) \text{ on } t \in [t_0, t_N], \text{ with } u(t_0) = u^0, \quad (1)$$

where $h : \mathbb{R}^d \times [t_0, t_N] \rightarrow \mathbb{R}^d$ is a smooth multivariate function, $u : [t_0, t_N] \rightarrow \mathbb{R}^d$ is the time dependent vector solution, and $u^0 \in \mathbb{R}^d$ are the initial values at t_0 . Parareal [3] solves (1) by dividing the timespan $[t_0, t_N]$ into N initial value problems

$$\frac{du_i}{dt} = h(u_i(t | U_i), t), \quad t \in [t_i, t_{i+1}], \quad u_i(t_i) = U_i, \text{ for } i = 0, \dots, N-1.$$

and solving them in parallel. To ensure continuity, the initial conditions U_i are iteratively updated every Parareal iterations k

$$U_i^k = \mathcal{G}(U_{i-1}^k) + \mathcal{F}(U_{i-1}^{k-1}) - \mathcal{G}(U_{i-1}^{k-1}), \quad i = 1, \dots, N-1, \quad (2)$$

where \mathcal{F} and \mathcal{G} are numerical solvers. \mathcal{F} is slow (hours, days), accurate, and always executed in *parallel*. \mathcal{G} is fast (seconds), inaccurate, and used to build the approximate solution *sequentially*. See Figure 2.

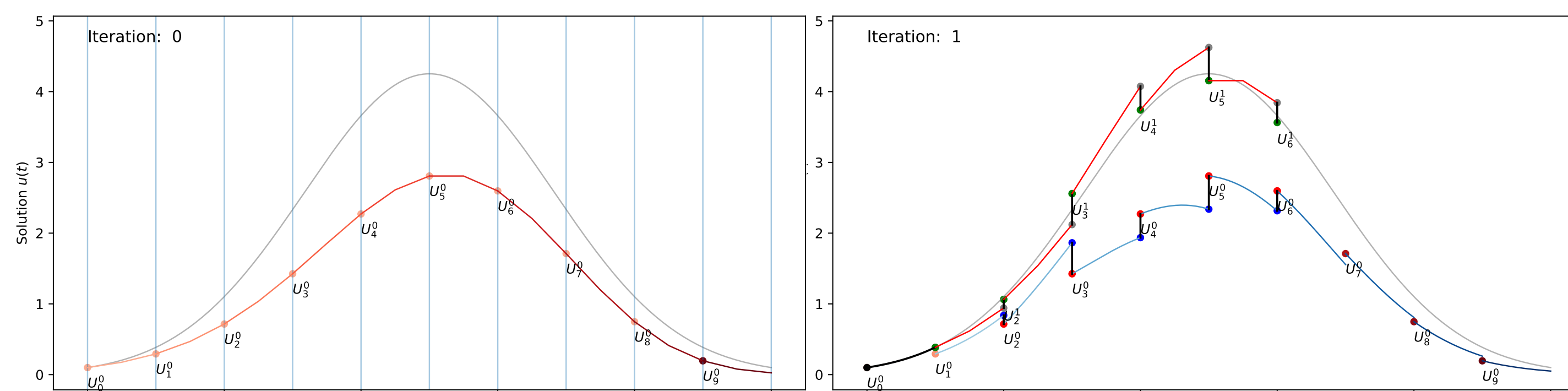


Figure 2: Parareal. Gray line, truth. Left, approximate initial solution \mathcal{G} at iteration $k = 0$. Right, parallel evaluations of \mathcal{F} (blue) and sequential evaluations of \mathcal{G} in (2) (red lines) for iteration $k = 1$. The green, gray, blue and red dots are U_i^k , $\mathcal{G}(U_{i-1}^k)$, $\mathcal{F}(U_{i-1}^{k-1})$, and $\mathcal{G}(U_{i-1}^{k-1})$ from (2).

In (2), Parareal uses data coming from the previous iteration $k-1$. GParareal [4] changes (2) to use current iteration information

$$U_i^k = \mathcal{F}(U_{i-1}^k) = (\mathcal{F} - \mathcal{G} + \mathcal{G})(U_{i-1}^k) = (\mathcal{F} - \mathcal{G})(U_{i-1}^k) + \mathcal{G}(U_{i-1}^k). \quad (3)$$

However, this would require a *serial* computation of $\mathcal{F}(U_{i-1}^k)$, defeating parallelization. Instead, Gaussian processes (GPs) are used to predict the correction term $\mathcal{F} - \mathcal{G}$ using the known (updated) initial condition U_{i-1}^k . At iteration $k > 0$, the GPs are trained on the dataset D_k composed of pairs of inputs U and outputs $y = (\mathcal{F} - \mathcal{G})(U)$:

$$D_k = \{(U_i^{j-1}, (\mathcal{F} - \mathcal{G})(U_i^{j-1})), i = 0, \dots, N-1, j = 1, \dots, k\}.$$

The GP posterior mean is used to predict $(\mathcal{F} - \mathcal{G})(U_{i-1}^k)$ in (3) as

$$m_{D_k}(U_{i-1}^k) = K(U_{i-1}^k, \mathbf{U})^T [K(\mathbf{U}, \mathbf{U}) + \sigma_n^2 I]^{-1} \mathbf{y}, \quad (4)$$

where $K(\mathbf{U}, \mathbf{U})$ is the covariance matrix. The matrix inversion in (4) is **computationally expensive** with a $O((Nk)^3)$ cost, cubic in the size of the dataset D_k at iteration k . This negatively affects speed-up (Figure 4) and makes GParareal unattractive for bigger N s. More intervals N allows for greater parallelization, hence the need for an alternative approach.

Nearest Neighbors GParareal New!

To overcome the computational bottleneck of GParareal, we reduce the dataset size, thereby decreasing the matrix inversion cost. As seen in Figure 3, *most points are far from the prediction point U_{i-1}^k* .

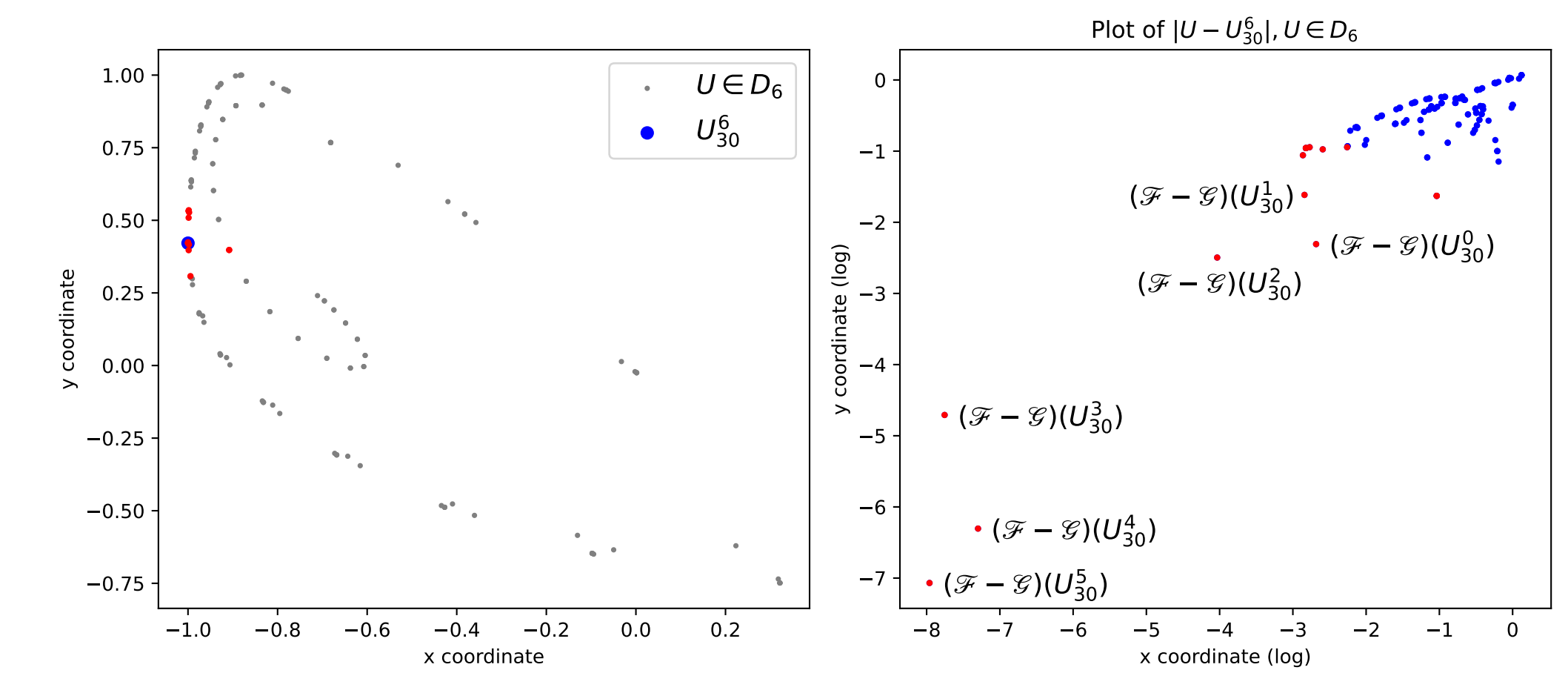


Figure 3: Left, a scatterplot of D_6 with the test observation $U_{i-1}^k = U_{30}^6$ (blue). In red are the $m = 15$ nearest neighbors to U_{30}^6 . Right, plot of the absolute (log) distance coordinate-wise between $U \in \mathbf{U}$ and U_{30}^6 .

Hence, for a prediction at U_{i-1}^k we can train the GP on a subset $D_{i-1,k} \subset D_k$ consisting of only m points, which we choose as the **nearest neighbors** to U_{i-1}^k (red dots in Figure 3). This is known in the literature as a nearest-neighbors GP (NNGP). Provided m is small, the computational complexity is *sensibly favorable* as the NNGP training cost is $O(Nm^3 + N \log(kN))$ at iteration k . The log component comes from data sorting operations.

Figure 4 shows the NN-GParareal speed-up, the ratio of running \mathcal{F} sequentially as opposed to using Parareal

$$\text{Speed-up} = T_{\text{serial}}/T_{\text{parall}},$$

where T_{\cdot} indicates wallclock runtime. The upper bound to the speed-up achievable by any algorithm converging in K steps is K/N . For low values of N , GParareal and NN-GParareal provide sensible speed-up. However, as the number of cores increases, GParareal performs worse than Parareal or fails to converge within reasonable time limits.

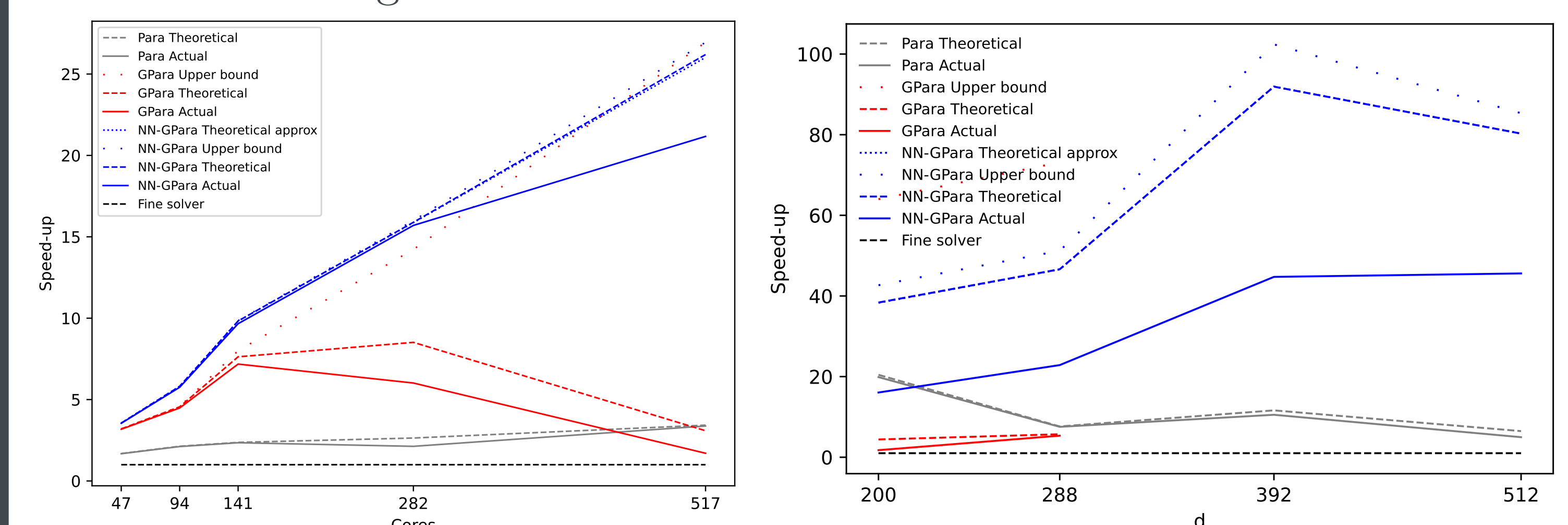


Figure 4: Speed-up for a 2D Hopf bifurcation ODE [5] (left) and FitzHugh-Nagumo 2D PDE [6] (right). Right, $N = 512$.

References

- (1) D. Samaddar, D. P. Coster et al., *Comput. Phys. Commun.*, 2019, **235**, 246–257.
- (2) O. Gorynina, F. Legoll et al., *arXiv preprint arXiv:2212.10508*, 2022.
- (3) J.-L. Lions, Y. Maday et al., *Comptes Rendus de l'Academie des Sci. I-Mathematics*, 2001, **332**, 661–668.
- (4) K. Pentland, M. Tamborrino et al., *Stat. Comput.*, 2023, **33**, 23.
- (5) R. Seydel, *Practical bifurcation and stability analysis*, Springer Science & Business Media, 2009, vol. 5.
- (6) B. Ambrosio and J.-P. Franoise, *Philos. Trans. Royal Soc. A: Math. Phys. Eng. Sci.*, 2009, **367**, 4863–4875.